JOURNAL OF AIRCRAFT
Vol. 42, No. 6, November–December 2005

Support Interference for a Maneuvering Delta Wing

G. S. Taylor* and I. Gursul†
University of Bath, Bath, England BA2 7AY, United Kingdom

The results of a recent investigation of support interference in dynamic wind-tunnel testing are presented. Particular emphasis has been focused on studying the interaction of vortices generated by delta wing models at high angle of attack with a support structure. A novel approach was used whereby the effects of time-varying vortex strength could be separated from the effects of the vortex–support interaction. With this approach, it was shown that the principal effect of support interference was to cause an upstream shift in the mean breakdown location, regardless of the form of motion or forcing frequency. The magnitude of the fluctuations in the breakdown location was shown to be dictated by support interference at low forcing frequencies, but by time-varying vortex strength effects at high frequencies. A number of important observations were also made of the vortex behavior at high forcing frequencies. In particular, a curious jumping behavior of the vortex breakdown location was observed. The presence of the support reduced the magnitude of the breakdown jump, but jumping was, nevertheless, observed in all of the cases considered at high enough forcing frequencies.

Nomenclature

b	=	wingspan, m
C_L	=	lift coefficient
c	=	wing root chord, m
f_e	=	frequency, Hz
Re_c	=	Reynolds number based on root chord
Sr	=	Strouhal number, fc/U_∞
T	=	time period of motion, $1/f$, s
t	=	time, s
U_∞	=	freestream velocity, m/s
x'_{BD}	=	chordwise breakdown location, m
x_{LE}	=	streamwise location of dummy support, m
α	=	angle of attack, deg
Γ	=	circulation, m^2/s
ε	=	distance between vortex core and support, m
Λ	=	wing sweep angle, deg
ξ	=	vorticity, rad/s

Introduction

THE conditions in wind-tunnel testing do not necessarily reflect those observed in free flight. The factors that affect experimental data collected from the wind- or water-tunnel environment include the following: the imposition of a boundary condition at the tunnel walls, changes in the velocity and pressure fields due to tunnel blockage, and interactions between the flow and the model support structure. Where delta wings are concerned, tunnel wall effects have been studied by a number of investigators, both experimentally[1,2] and computationally.[3–6] The influence of blockage in a flow is a standard topic covered in many textbooks[7] and reference sources.[8] However, the effects of support structure interference are less well understood. This is particularly true in relation to testing of delta wing geometries.

Although a number of different support structures have been developed over the years,[9] that, in many cases, can reduce interference effects to a minimum, it is impossible to remove these effects entirely. Thus, it is important that any influence that the support structure has on the flow, particularly in the region of interest, is recognized and suitably accounted for. Support interference effects were first studied using bodies of revolution to simulate an aircraft,[9–11] and representative conventional aircraft configurations have also been considered.[12] Flows over delta wings are characterized by the existence of strong primary leading-edge vortices, and it is the focus of the current investigation to study the interaction of these vortices with a representative dynamic support structure.

Early work in this field demonstrated that breakdown of the leading-edge vortex over a 75-deg cropped delta wing could be moved upstream by 40% of the chord length by placing an obstacle in line with the vortex core,[13] thereby demonstrating the potential for support interference of this nature. Further experiments using a delta wing aircraft configuration,[12] and subsequent discussion,[10] showed that support interference may not only result in premature breakdown, but under certain conditions may result in the premature breakdown occurring over the wing surface, causing a reduction of the lift measured over the model.

The potential for support interference becomes even more significant in dynamic tests. In this case, the supports used tend to be bulky, both to house the mechanisms required for the model movement and to ensure that unwanted vibrations are kept to a minimum, and there tends to be less flexibility in terms of their placement relative to the test model. Dynamic support interference relating to aircraft configurations has been the subject of many investigations,[9,10,14–17] and these studies have confirmed the urgent need for quantitative data. The most recent relevant investigation in this specific area is that by Ericsson and Beyers,[18] which reviews literature relating to the factors affecting the breakdown of leading-edge vortices generated by a 70-deg delta wing. The effects of model size, test facility, camber, and Reynolds number scaling on support interference were studied, with the conclusion that attention must be paid to all of these factors when designing experiments.

A recent study[19] showed that a dummy support structure representative in size of a typical dynamic support can induce breakdown a significant distance upstream of its expected location in static testing. Some important parameters were identified, including the geometry of the support, the distance between the trailing edge of the wing and the support, and the lateral distance between the support and the vortex axis. Static hysteresis of vortex breakdown location was also identified. For the same support position, the location of the breakdown differed depending on whether the support was being stepped toward or away from the vortex core; similar hysteresis behavior has also been noted in response to quasi-static variation of the swirl angle in computational simulations[20] and of the pitch angle in experiments[21] using a delta wing. In Ref. 19, the results of some preliminary dynamic tests that indicated that the breakdown response

Received 19 July 2004; revision received 28 September 2004; accepted for publication 28 September 2004.

*Postdoctoral Research Associate, Department of Mechanical Engineering; currently at Atkins Aviation and Defence Systems, Bristol BS32 4SD, U.K. Member AIAA.

†Professor of Aerospace Engineering, Department of Mechanical Engineering. Associate Fellow AIAA.

to a dummy support oscillating laterally was similar to that of a low-pass filter is also presented, with increasing frequency of oscillation resulting in smaller amplitude fluctuations of breakdown location.

The aim of this paper is to present the results of our continued research into dynamic support interference. Dummy support structures were used to represent a dynamic support structure, and in the current experiments, both a moving support and a moving model were used. Flow visualization and velocity and force measurements document the response of the leading-edge vortices generated over delta wings to this form of interference.

Methodology

All experiments were conducted in the water-tunnel facility at the University of Bath. The tunnel has a working section of $0.38 \times 0.51 \times 1.52$ m, which can provide velocities in the range from 0 to 0.45 m/s with a turbulence intensity of less than 1% rms, through a horizontal, closed-circuit continuous flow system. Simple delta wings were chosen for this investigation because they generate a reasonably simple and predictable vortical flowfield for which interactions with support structures could be studied. Three models were tested, having sweep angles $\Lambda = 70$, 75, and 80 deg. The test models had a thickness of 5 mm and chord lengths ranging from 137 to 250 mm, giving thickness-to-chord ratios of 3.6, 2.7 and 2%, respectively. All models incorporated a sharp leading edge formed by beveling the pressure surface by 30 deg; the trailing edge was square. Maximum blockage was approximately 3.7% for the $\Lambda = 80$-deg wing at $\alpha = 40$ deg. Flow visualization models were constructed from an aluminium alloy and incorporated embedded dye tubes to enable transport of the dye to the wing apex; these models were also used for particle image velocimetry (PIV) measurements. For force measurements, identical models were constructed from PVC to reduce pre-loading of the balance load cells.

As in previous studies,[19,22] the support structure interference was modeled using a dummy support structure placed in the wake of the delta wing models (Fig. 1). The location of the dummy support was varied both quasi statically and dynamically, and the effect on the breakdown location of the leading-edge vortices was studied. Two dummy support geometries were tested, one of circular cross section, $d = 12$ mm, and the other a flat plate of streamwise length, $l = 48$ mm. An overview of the setup is shown in Fig. 1. The dummy supports were placed downstream of the delta wing at a location relative to the wing defined by the parameters x_{LE} and ε, the streamwise distance of the leading edge of the support from the trailing edge of the wing, and the lateral distance between the center of the support and the vortex axis, respectively. For all of the cases considered in this study, the parameter x_{LE} was fixed at one-quarter of the chord length of the wing being tested, that is, $x_{\mathrm{LE}} = c/4$, whereas ε was varied sinusoidally, and the effect on breakdown location and lift force was measured. The location of the breakdown, measured from the apex in a plane parallel to the wing surface, is x'_{BD}.

In dynamic testing, an approach was adopted that would allow the effect of time-dependent vortex strength to be considered separately from that of support interference. Initial dynamic tests were performed using a static wing with the dummy support oscillating in its wake. In this way, the effect of dynamic interference between the support and a vortex of constant strength was studied. Following this, the more complicated case of an oscillating wing was considered, allowing the full dynamic interaction to be considered. The form of dynamic motion chosen for this research was a lateral motion inducing a periodically varying effective sideslip. The dummy support or wing was oscillated by using a hydraulic actuator placed above the tunnel, as shown in Fig. 2, which was controlled via a desktop personal computer. A feedback signal from a linear potentiometer provided precise positioning of the model.

The oscillating motion for both the moving wing and the moving support cases is described by the equation

$$\varepsilon/b = \varepsilon_0/b + (\varepsilon_1/b)\cos(2\pi f t) \tag{1}$$

where ε_0/b is the mean support location, ε_1/b is the amplitude, and f is the frequency of the motion. The lateral location of the support ε is measured from the location of the undisturbed vortex core location, positive toward the wing tip. Three forms of this oscillating motion were considered to provide an understanding of the relative influences of amplitude and the offset on the support–vortex interaction. The different time histories of the motions considered are shown in Fig. 3; a discussion of the selection of these waveforms is given hereafter. Reduced frequencies in the range $0.015 < Sr < 0.5$ were considered, representing a large range of possible aircraft maneuvering speeds. The oscillations were allowed to continue for at least 100 convective timescales ($100c/U_\infty$) before measurements were taken to ensure that all transients had died out.

Measurement of the vortex breakdown location was achieved by elucidating the vortex core by means of dye flow visualization. This was achieved using food coloring diluted 1:4 with tap water, which

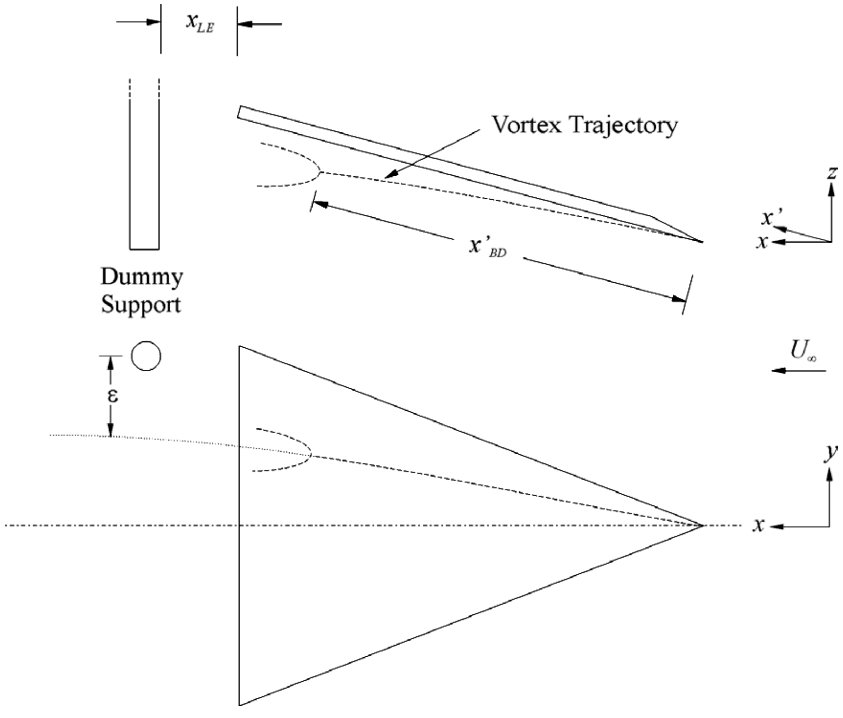

Fig. 1 Overview of experimental setup.

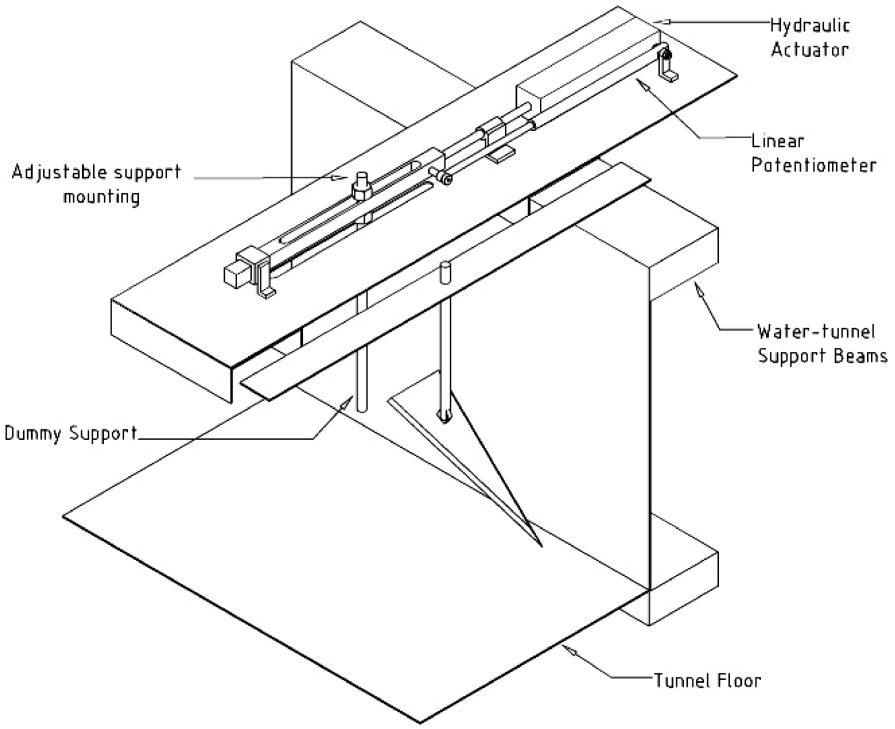

Fig. 2 Schematic of rig used to generate oscillating motions of wing.

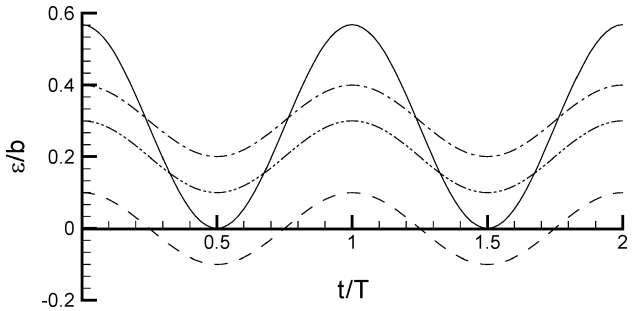

Fig. 3 Time history of the oscillatory dummy support and wing motions: ——, waveform A, $\varepsilon_0/b = 0.285$, and $\varepsilon_1/b = 0.285$; – – –, waveform B, $\varepsilon_0/b = 0.0$ and $\varepsilon_1/b = 0.1$; –·–, waveform C, $\varepsilon_0/b = 0.3$ and $\varepsilon_1/b = 0.1$ (cylindrical support); and –··–, waveform C, $\varepsilon_0/b = 0.2$ and $\varepsilon_1/b = 0.1$ (flat-plate support).

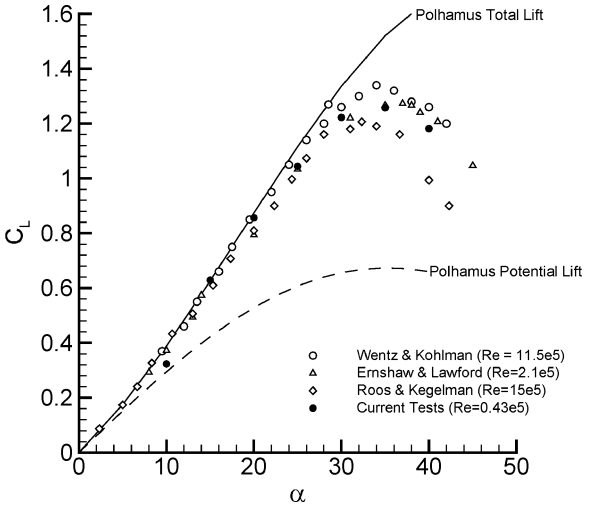

Fig. 4 Comparison of C_L for $\Lambda = 70$ deg delta with experimental and theoretical data from literature.

was injected under pressure into the flow at a suitable velocity. Flow visualization images were captured using a digital video camera with a capture rate of 25 frames per second and a resolution of 570,000 pixels. Breakdown locations were measured from these images with an uncertainty of around $0.01c$. For flow visualization and force balance measurements, a flow velocity of $U_\infty = 0.1$ m/s was selected, which corresponds to Reynolds numbers based on root chord in the range $Re_c = 1.4 \times 10^4$–2.5×10^4.

For the experiments with stationary wings and oscillating dummy supports only, lift forces were measured using a pair of load cells placed along the axis of the tunnel, connected to the test model via a crossbar and sting arrangement constructed from a carbon composite material.[22] The load cells had a minimum and maximum measurable lift force of approximately 0.0012 and 2.5 N, respectively. Because of limitations of the balance, force measurements were not conducted for moving wing tests. For the range of lift forces considered in this investigation, balance uncertainty was estimated to be less than 1% at $C_{L\max}$. Figure 4 shows a comparison of lift forces measured for a 70-deg delta wing with data presented in the literature, along with the theoretical prediction by the Polhamus leading-edge suction (LES) theory.[23] Over the range of incidences considered, the data show excellent agreement.

Measurements of velocities in the crossflow plane were undertaken using PIV. Illumination of the crossflow plane was achieved using a pair of pulsed miniature Nd:YAG lasers with a maximum energy of 120 mJ per pulse situated beneath the water tunnel. Digital images were captured with a charge-coupled device camera with a resolution of 2048×2048 pixels and a maximum capture rate of 3.75 measurements per second in cross correlation. The flow was seeded with hollow glass spheres of mean diameter 4 μm. Synchronizing the support/model motion with the PIV capture allowed phase-locked PIV measurements to be made. For PIV and lift force measurements, a flow velocity of $U_\infty = 0.30$ m/s was selected to ensure minimum settling of particles during the test and a greater magnitude of lift forces, resulting in Reynolds numbers in the range $Re_c = 4.1 \times 10^4$–7.5×10^4.

Results

Before discussing the current results, a brief review of the different forms of dynamic motion tested is merited. In a previous investigation,[19] it was found that the support structure needed to not be located directly in line with the vortex core to affect the breakdown location. For each of the support geometries, the maximum

lateral distance from which the dummy support could affect the breakdown location in static testing was defined by the parameter $\varepsilon_{\text{crit}}$. This parameter was then used to select values of mean support location and amplitude of the oscillation that define the dynamic motion. In this way, dynamic motions of particular interest were identified.

In the first form of motion (waveform A in Fig. 3), a large-amplitude motion is considered. In this form of motion, the support oscillates sinusoidally between $\varepsilon = 0$, that is, in line with the vortex core, and $\varepsilon > \varepsilon_{\text{crit}}$, so that during each cycle the support moves sufficiently far from the vortex core to allow the breakdown to begin to recover its natural location, before being affected during the remaining phase of the cycle. In the second form of motion (wave B), a small amplitude is considered with a mean at $\varepsilon = 0$ and $|\varepsilon_{\max}| < \varepsilon_{\text{crit}}$, such that the support is always within its range of influence of the vortex core. Finally, in the third form of motion (wave C), a small-amplitude motion was considered, in which the mean support location was equal to $\varepsilon_{\text{crit}}$ for the relevant support.

Moving Support Tests

The effect of an oscillating dummy support on breakdown location was first considered. By the use of this method, the effects of time-varying vortex strength could be removed, leaving only the effect of support interference. The effect of varying ε sinusoidally by moving a dummy support downstream of an 80-deg delta wing set at $\alpha = 30$ deg is shown in Fig. 5 for waveform A (Fig. 3) and the flat-plate support placed at $x_{\text{LE}} = c/4$. In all of the cases presented here, the visualized vortex was on the windward side of the model during the initial phase of the cycle, that is, during the decreasing ε/b phase. For the candidate wing configuration, breakdown was not observed in the static, nonmaneuvering case. Thus, the effect of oscillating the dummy support was to provoke the onset of breakdown. In addition, at low frequencies, the support motion also induced significant fluctuations of breakdown location, which decreased in amplitude as the forcing frequency was increased. For further discussion of these results, see Refs. 19 and 22.

Ultimately, it was the lift generated by the wing that was of greatest interest, and it was important that the effect of support interference was quantified in this respect. To achieve this, force measurements were first undertaken for a range of wings of varying sweep angle in the static case, that is, for fixed ε. Figure 6 shows a comparisons of the variation of lift coefficient measured for the $\Lambda = 70$-, 75-, and 80-deg wings both in the presence and absence of the cylindrical support in the static case. In all of these cases, the support, when present, was located at $(x_{\text{LE}}, \varepsilon) = (c/4, 0)$. In the prestall region, in both the natural and forced cases and for all of the wings, lift was comparable with that predicted by Polhamus's LES theory.[23] In the stall region, lift does not reach the theoretical maximum due to the onset of vortex breakdown and the resulting decrease in the vortex lift contribution to total lift. Although this is to be expected in the absence of support interference, above a certain incidence a marked additional drop in lift was noted when the dummy support was present. It was hypothesized that this lift detriment was a result of the premature onset of vortex breakdown over the wing surface due to the presence of the support.

For the 70- and 75-deg wings, the onset of this lift detriment occurred at roughly the same incidence, $\alpha \approx 15$ deg. In both of these cases, a gradual increase of the lift deficit in the presence of the support was noted above this incidence. For the 80-deg wing though, a much more sudden break in the lift curve was observed at around $\alpha \approx 25$ deg. Furthermore, the magnitude of the lift detriment was larger in this case, with $C_{L\max}$ in the presence of the support being roughly 84% of that in the natural case for the 80-deg wing, compared with 90 and 91% for the 75- and 70-deg wings, respectively. This is to be expected because as the sweep angle is increased, Polhamus's theory predicts that the contribution to total lift by the vortex lift component increases.[23]

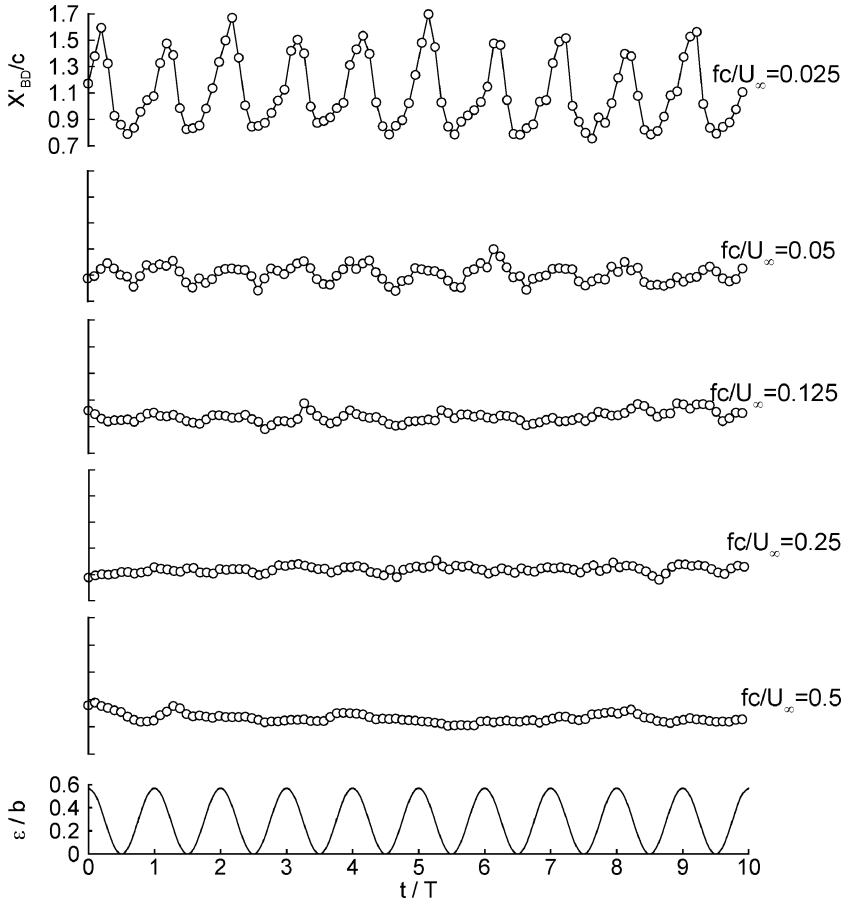

Fig. 5 Breakdown response to oscillatory support motion; waveform A, flat-plate support.

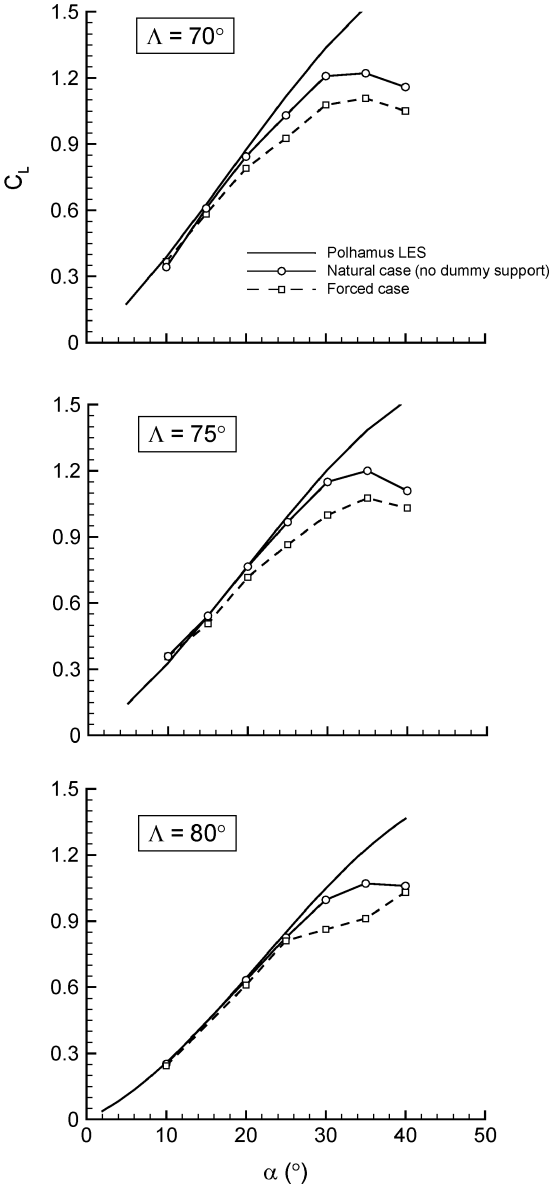

Fig. 6 Variation of lift force with incidence for 70-, 75- and 80-deg delta wings in the absence and presence of 12-mm cylindrical support.

The effect of an oscillating dummy support on the measured lift was considered next. For the $\Lambda = 80$ deg wing, incidences of $\alpha = 30$ and 35 deg were chosen as representative cases of particular interest, as identified by flow visualizations[22]: In the first case, breakdown occurs naturally downstream of the trailing edge, but is known to be particularly sensitive to dummy support location; in the latter case, the breakdown occurs over the wing surface in the natural case.

For these incidences, the three oscillating waveforms outlined earlier (A, B, and C in Fig. 3) were considered for both dummy support geometries. For brevity, only a single example of the lift force time history is presented herein and is shown in Fig. 7. Figure 7 shows the variation of C_L with normalized time t/T for the 80-deg wing in the presence of the large-amplitude oscillation (waveform A) of the flat-plate dummy support. The lift force response takes a similar form to that of the breakdown location (Fig. 5), with the reducing of the frequency of the support motion resulting in larger-amplitude force oscillations; this was also true for oscillation of the cylindrical support.[22] However, on closer inspection, a subtlety of the response can be discerned. For the response shown in Fig. 7, the lift force fluctuation exhibited peak values that appeared to be "capped," that is, the lift force reaches a value that does not change significantly until it reduces again with the returning support. It is expected that this behavior was a direct result of the large-amplitude fluctuations of the breakdown location past the trailing edge, as observed during flow visualization experiments (Fig. 5). In other words, as the support moves away from the vortex core, the breakdown is allowed to move downstream, and the lift generated by the wing, therefore, increases. However, when the breakdown has moved aft of the trailing edge, it cannot affect the lift generation, and the lift force fluctuations appear to reach a maximum.

To summarize the lift force response over a range of frequencies, the peak cross-spectral magnitude between C_L and ε was considered. This gives a measure of the dependence of the lift force signal on the support location; if the variations in lift force are a result of the support movement as expected, one would expect a high-magnitude peak in the cross spectrum, whereas low dependence will result only in a background correlation level. These data are presented in Fig. 8 for the 80-deg wing at $\alpha = 30$ and 35 deg. For both support geometries, the largest-amplitude motion resulted in the greatest coherence between the signals at all frequencies, as was expected. The response to the small-amplitude motions was a little more complex, especially at higher frequencies when the coherence between the signals was at a minimum. At the lowest frequencies, it was the small-amplitude motion offset from the vortex core (wave C) that induced the strongest response, compared to the oscillation about the vortex core location (wave B). Previously, in static testing,[19] it was shown that for $|\varepsilon| < \varepsilon_{\text{crit}}$, the breakdown location was only a weak function of ε. Outside of this range, for $|\varepsilon| > \varepsilon_{\text{crit}}$, the breakdown location could no longer be affected by the presence of the support and, over time, moves to its natural location. This explains the current observations that wave C induces the strongest response compared with wave B because for wave B the support is always affecting the breakdown location, whereas for wave C the support is only affecting the breakdown location for part of the cycle.

There is a degree of spread in the data for the small-amplitude oscillations at high frequencies, most likely a result of the greater noise in the signal and resulting small coherence between the signals. Further results have shown that there is little difference between the breakdown response over 70- and 80-deg wings, indicating that in dynamic testing the effect of sweep angle is small.[22]

This section has elucidated some of the characteristics of support interference in dynamic testing in the absence of time-varying vortex strength effects. It has been shown that support interference is a factor throughout the range of frequencies tested, although the magnitude of the fluctuations of breakdown location reduces as the frequency is increased. An explanation of this behavior has been suggested previously,[19,22] that is based on the time lag of vortex breakdown location in unsteady flows.[24] The results have shown that the lift force response to an oscillating dummy support is similar to that of the breakdown location.

Oscillating Wing

The focus now shifts to considering support interference effects in the presence of time-varying vortex strength effects. For this case, it was not possible to measure lift forces due to rig constraints, and the discussion of the response is limited to the effect of the dynamic motion on the breakdown location. Figure 9 shows the breakdown response to a moving wing of 80-deg leading-edge sweep at 30-deg incidence with a static dummy support, in this case the flat-plate support, placed at $x_{\text{LE}} = c/4$. A similar breakdown response was observed at low frequencies as in the moving support case; the amplitude of breakdown fluctuations decreased with increasing frequency, whereas the mean breakdown location moved upstream. However, at the highest frequencies, the amplitude of the breakdown fluctuations began to increase.

The peak cross-spectral magnitude between ε and x_{BD}, as a function of frequency for each case, is shown in Fig. 10. Figure 10 highlights some important differences between the moving support and moving wing cases. In the moving support case, the correlation between support and breakdown locations decreased as the forcing frequency was increased, giving the expected low-pass filter response described earlier.[19] In the moving wing case, the breakdown response was similar to the moving support case at low

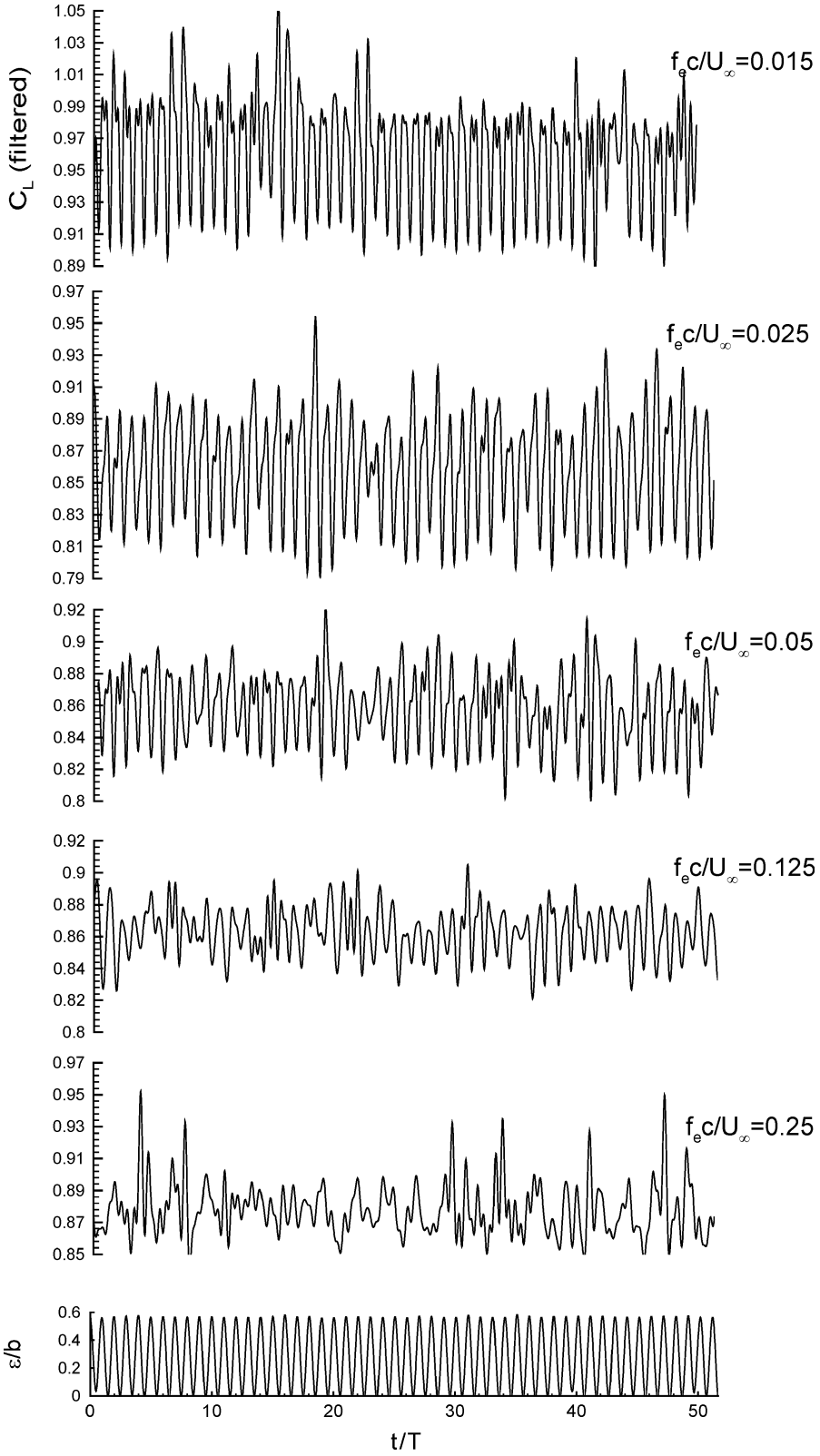

Fig. 7 Lift force response; waveform A, flat-plate support.

frequencies of wing motion. However, as the frequency was increased above a certain critical level, the correlation between the signals started to increase again, demonstrating how the influence of changes in vortex strength due to the wing motion begins to dominate the breakdown process rather than the presence of the support, as is the case at low frequencies.

Also shown in Fig. 10 is the breakdown response to an oscillating wing in the absence of a dummy support for waveform A at the two highest frequencies. The time histories of breakdown location for these cases are shown in Fig. 11. Note again that in the static, unobstructed case breakdown does not occur for this configuration, and oscillating the wing at frequencies below $Sr = 0.25$ could not affect this absence of breakdown. However, for $Sr \geq 0.25$ the motion of the wing alone was sufficient to induce vortex breakdown for this configuration. At the lowest frequency where this behavior was observed ($Sr = 0.25$) some breaks in the time history were noted due

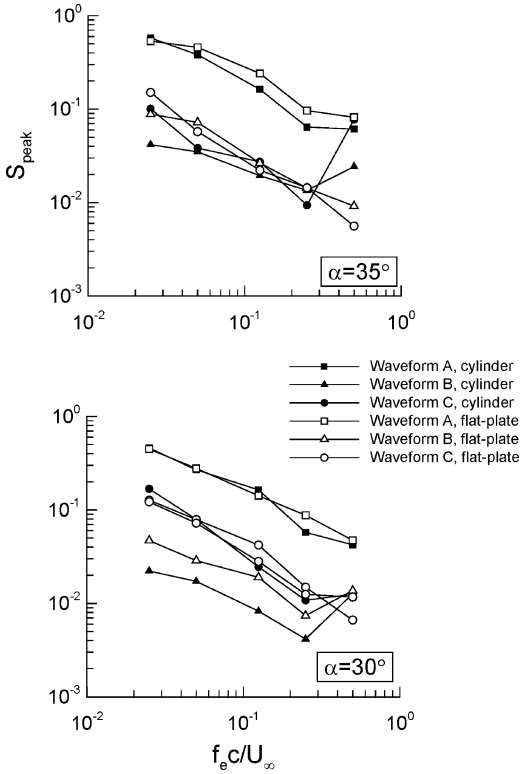

Fig. 8 Variation of magnitude of dominant cross-spectral density of lift force and ε/b for the 80-deg wing.

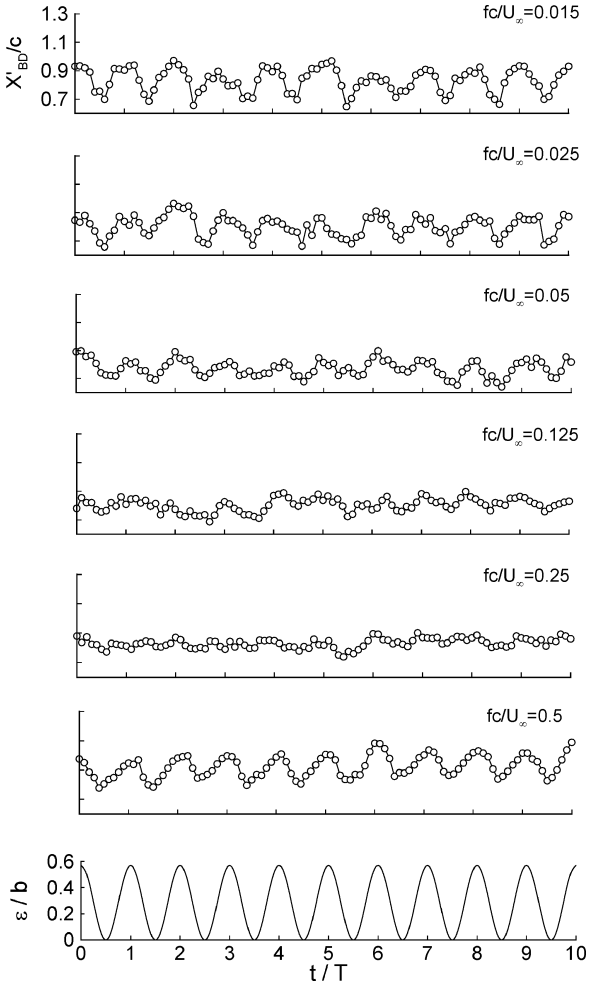

Fig. 9 Breakdown response to oscillatory wing motion; waveform A, flat-plate support.

to the vortex regaining its unbroken state while on the leeward side of the model; for the higher frequency ($Sr = 0.5$), no breaks in the time history were observed. Increasing the frequency also induced a forward movement of the mean breakdown location. Note that waveforms B and C, which are smaller-amplitude motions, did not induce breakdown at any frequency in the absence of a dummy support.

In Fig. 10, note that the dominant spectral peaks in the absence of a support were larger than those in the presence of a support. This may be explained by comparing the time histories presented in Figs. 9 and 11. In the absence of a support (Fig. 11), the breakdown location is free to transit the trailing edge, whereas in the presence of a support (Fig. 9), the breakdown is constrained to $x'_{BD}/c < 1$. These results indicate that there are fundamental differences between the character of the support interference in the cases of a moving wing and a moving support. In the moving support case, and in the absence of variations of vortex strength, fluctuations in the breakdown location are a sole result of interference between the vortex and the dummy support structure. In the more realistic moving wing case, variations in vortex strength through the cycle significantly increase the complexity of the response.

An interesting feature of the breakdown response was the discontinuity in the breakdown location at various points in the cycle. In Fig. 11, at approximately $t/T = 0.4$ in each cycle, the breakdown was seen to move rapidly upstream by a distance of approximately $0.5c$, a behavior that will subsequently be referred to as breakdown-jumping. The position of the breakdown jump was not affected by forcing frequency for the two values that induced breakdown. This breakdown jumping, although to a lesser degree, was also noted in the presence of a dummy support, as indicated at the higher frequencies in Fig. 9.

Not only was the location of breakdown significantly influenced by the motion of the wing, but the trajectory of the vortices relative to the wing was also altered. Figure 12 shows images captured at $t/T = 0.25$ and 0.75, the two points in each period at which the lateral velocity of the wing was greatest in either direction. When the visualized vortex was on the windward side of the wing ($t/T = 0.25$), the vortex moved slightly closer to the wing compared to the static case and shifted toward the wing centerline. When on

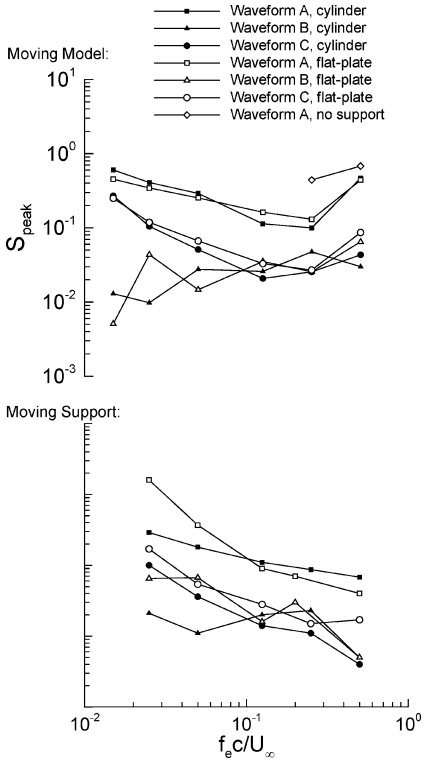

Fig. 10 Variation of magnitude of dominant cross-spectral density of breakdown location with wing.

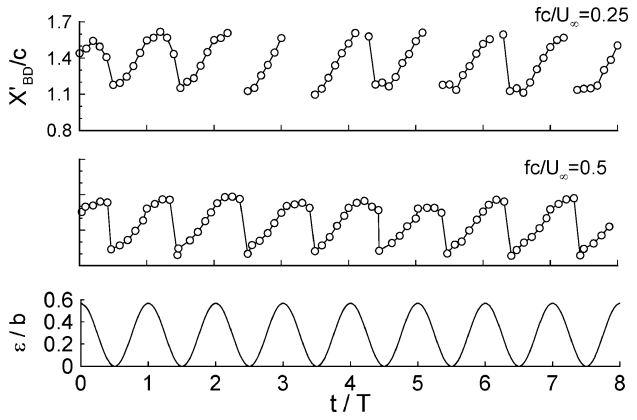

Fig. 11 Vortex breakdown response to wing motion oscillating laterally in the absence of a dummy support.

the windward side ($t/T = 0.75$), the vortex moved away from the wing surface and the centerline. These observations are consistent with observations of vortex trajectories over a delta wing in static sideslip.[25,26]

There is a point at each extreme of motion at which the vortex must effectively change its orientation on the wing and move from being on the leeward to the windward side of the wing, or vice versa. Evidence from flow visualization experiments has indicated that this transitional phase has a significant influence on the vortices. Figure 13 shows a sequence of flow visualization images that demonstrate the large deflections experienced by the vortex in response to a large amplitude motion of the wing at the high frequency, $Sr = 0.5$. At the beginning of the sequence ($t/T = 0$), the visualized vortex was on the leeside of the model, and, as expected from Fig. 12, the vortex was lifted away from the suction surface of the wing. However, at $t/T = -0.2$, a small "kink" in the trajectory of the vortex is observed just aft of the apex of the wing; the position is indicated by an arrow in Fig. 13. As the wing continued its motion,

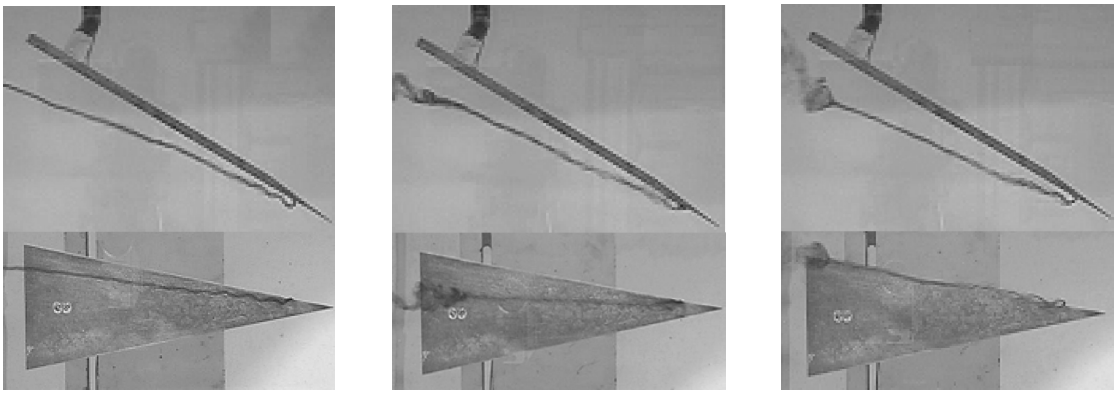

a) Static wing **b) Oscillating wing $t/T = 0.25$, $V = V_{max}$** **c) Oscillating wing $t/T = 0.75$, $V = -V_{max}$**

Fig. 12 Lateral and vertical deflection of the vortex trajectory due to wing motion in the presence of dummy support at $x_{LE} = c/4$; waveform A, $Sr = 0.5$.

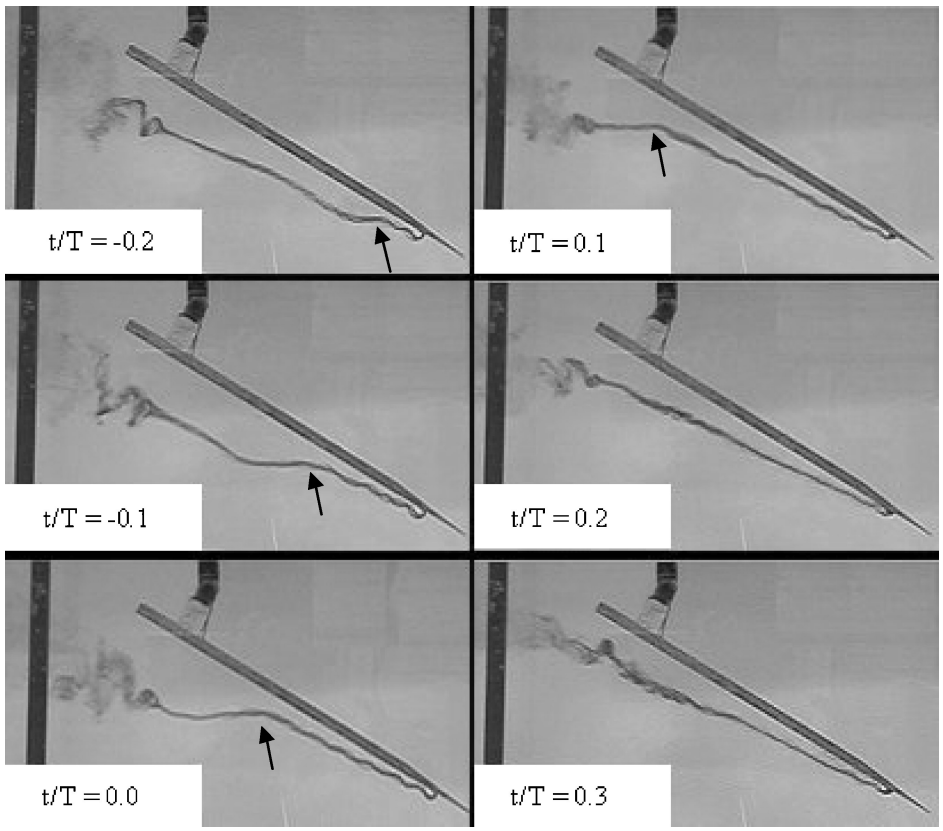

Fig. 13 Unsteadiness in the vortex filament resulting from change of direction of wing at extreme of motion.

this kink moved downstream and grew significantly. At $t/T = 0$, the vortex was seen to bend through an angle of approximately 30 deg. By the time the wing had reached $t/T = 0.2$ into the next cycle, the kink in the vortex trajectory had been washed out. It is thought that this large instability of the vortex is a result of the change in the direction of the wing motion. Because a the high frequency of motion, the change from one orientation to the next occurs rapidly, and the realignment of the vortex is, therefore, similarly rapid, and a kink is formed in the vortex.

As the time series shown in Fig. 13 progresses, a rapid movement of the breakdown location in the upstream direction was observed, and at $t/T = 0.2$ the vortex undergoes what may be described as a double breakdown as the breakdown undergoes a step change in its location. Upstream of the clearly defined breakdown at $x'_{BD}/c \approx 0.9$, at approximately $0.6c$, there is a region of turbulence that will develop into the primary breakdown at $t/T = 0.3$. It almost appears as if two separate breakdowns exist in the vortex simultaneously. Note that the double-breakdown structure

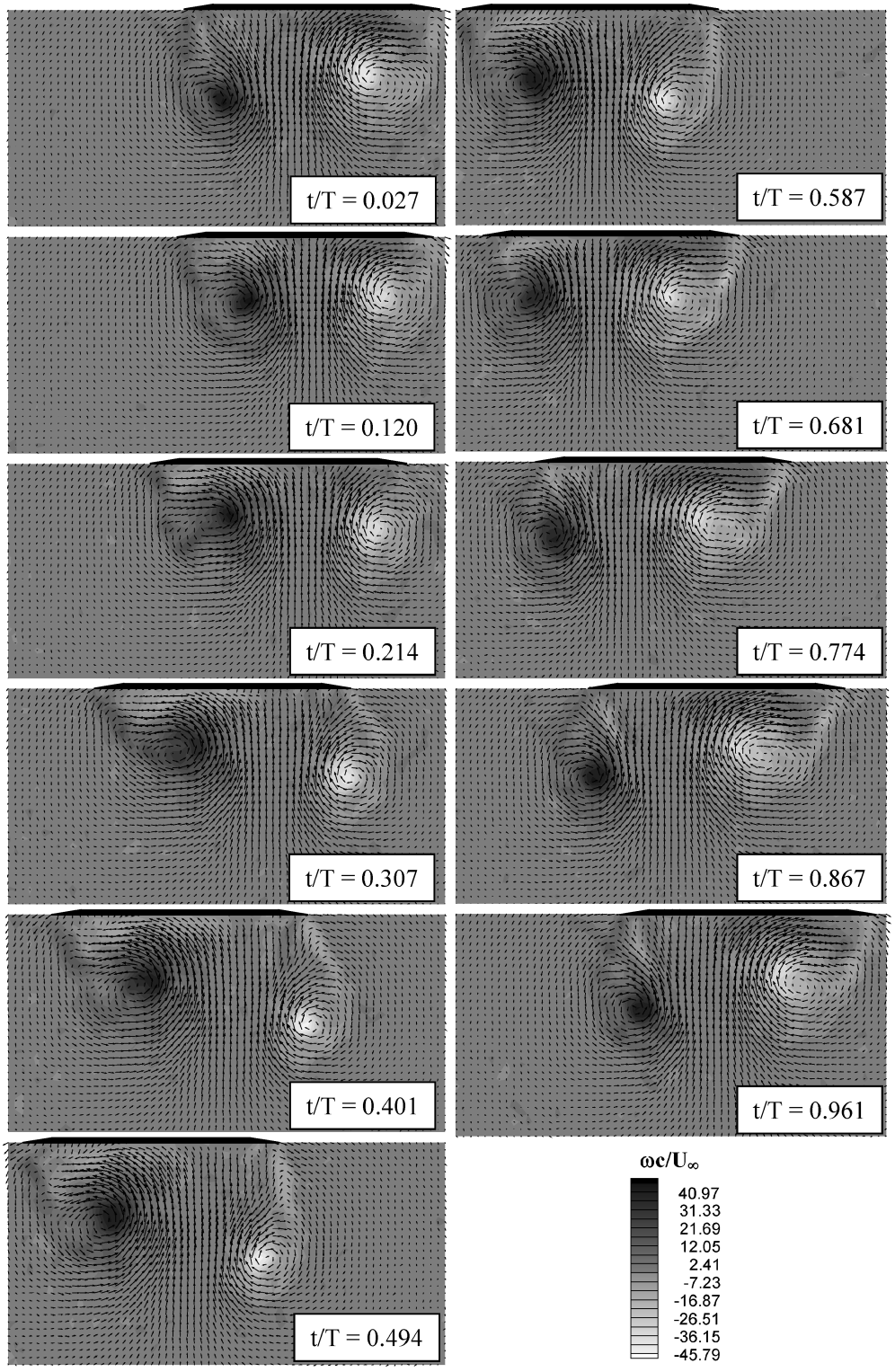

Fig. 14 Response of vortices to oscillatory wing motion; velocity vectors plotted on contours of axial vorticity in the crossflow plane at $x/c = 0.8$, $f_e c/U_\infty = 0.5$.

was previously[27] observed in steady conditions, when the external pressure gradient was manipulated. The breakdown-jumping and double-breakdown phenomena have also been noted in transient tests.[22,28]

It is difficult to estimate how these forms of unsteadiness may affect the occurrence of breakdown. Hall[29] showed how an external pressure gradient might be amplified along a vortex core, ultimately forming a stagnation point characteristic of vortex breakdown. It is clear from Fig. 13 that a degree of unsteadiness is associated with the period in which the lateral motion of the wing is decelerating, and this kinking of the vortex filament is likely to be accompanied by changes in the streamwise pressure gradient. It is, therefore, likely that these changes to the pressure field would have an effect on the breakdown location and may even be a contributing factor to the jumping of the breakdown location, which occurs shortly following the beginning of each new period of motion.

Similar jumping of the vortex breakdown location has also been observed over delta wings subjected to an oscillating freestream velocity.[30] In that case, the jumping of the breakdown location was only observed in the region of the trailing edge; when the breakdown was always over the wing surface the magnitude of the breakdown fluctuations was much smaller. Gursul and Ho[30] conducted laser Doppler velocimetry measurements of the vortex to enable calculations of both swirl angle and vortex strength to be made. Gursul and Ho[30] went on to show that their observations of the breakdown jump could not be attributable to changes in vortex strength. It is widely agreed that there are only two principal factors affecting the location of the breakdown[29,31]: the amount of swirl and the presence or otherwise of an adverse pressure gradient. It was, therefore, concluded that the movement of breakdown location was a result of changes in the adverse pressure gradient, presumably associated with the trailing edge. In the current investigation, however, the changes in vortex strength were generated by the variation of the effective sideslip of the wing.

To determine the relative significance of the changes in vortex strength to the breakdown-jumping phenomenon, PIV was used to document quantitatively the time dependency of the vortex strength and trajectory observations presented earlier. The crossflow velocity field was studied at $x/c = 0.8$ at the highest forcing frequency, $f_e c/U_\infty = 0.5$. Figure 14 shows phase-averaged velocity vectors plotted on contours of constant vorticity at 11 points during the cycle. Near the beginning of the cycle ($t/T = 0.120$), the size and strength of the leading-edge vortices were approximately equal, with any differences being remnants of the preceding cycle. As the wing continued its motion, the windward vortex (on the left of the image) began to strengthen and move toward the centreline of the wing. As it did so, the vortex flattened and shifted slightly toward the surface of the wing. During this half of the cycle, the leeward vortex (on the right of the image) moved away from the model centerline and lifted significantly from the surface of the wing. At $t/T = 0.681$ the vortices once again became approximately equal in strength and size, indicating a phase lag between the model motion and the response of the vortices. At this point in the cycle the vortices had swapped their orientations, with the former windward vortex now becoming the leeward vortex and vice versa.

The phase-averaged movement of the vortex core in this plane, relative to the wing surface, is shown in Fig. 15. In Fig. 15, (0, 0) represents, at $x/c = 0.8$, a point on the surface of the wing at its centerline, and the axes are normalized by the local semispan s. The data confirm the results of the visualizations presented in Fig. 12 and provide additional quantitative information about the movement of the vortex during each period. In terms of the vertical and horizontal movement of the vortex core, note that the most significant effect occurs from around halfway through the leeward phase of the cycle until the beginning of the windward phase. The origin of the unsteadiness in the vortex filament shown in Fig. 13 is not difficult to imagine considering that the vortex is attempting to recover from the large deflections gained during the leeward phase of the cycle. The deflection of the vortex during the windward and initial leeward phases of motion are small, perhaps because, in the windward case at least, the boundary condition imposed by the wing surface acts

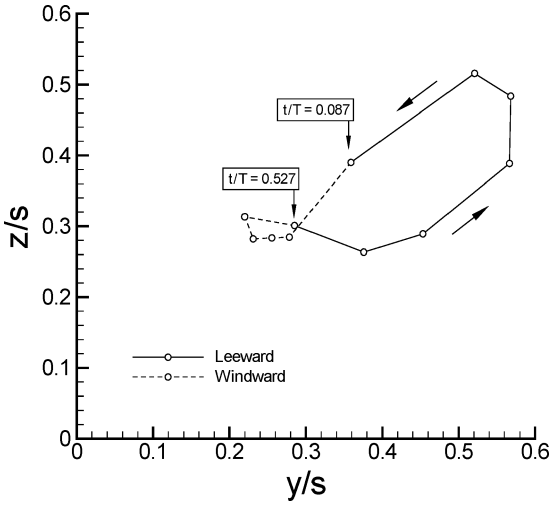

Fig. 15 Variation of vortex core location relative to wing surface; (0, 0) represents the point lying on the wing surface at its centerline at $x/c = 0.8$.

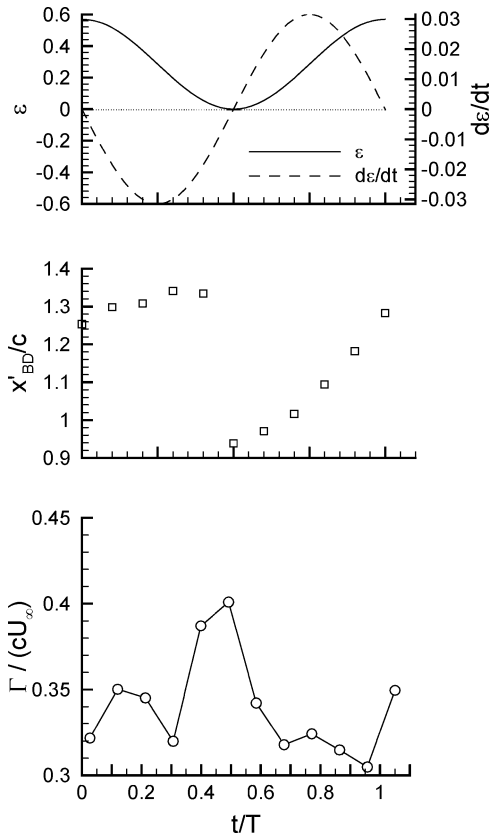

Fig. 16 Variation of phase-averaged circulation with time at $h/b = 0.227$, compared with phase-averaged breakdown location x'_{BD}/c and location ε and velocity $d\varepsilon/dt$ of wing through cycle.

to constrain the movement of the vortex core; this is not the case during the leeward phase, and the vortex core is allowed to wonder freely away from the wing surface.

Figure 16 shows how the strength of the vortex varied through a single period and compares this with the velocity and location of the wing at each point and with the location of the breakdown. The strength of the vortices is presented in terms of phase-averaged circulation normalized by root chord and freestream velocity and was calculated from the PIV data presented earlier around a square path of side length $h/b = 0.227$ centered on the vortex core. At the start of the cycle, the vortex was seen to strengthen, reaching

its peak strength of $\Gamma/cU_\infty \approx 0.4$ at $t/T = 0.49$, almost exactly halfway through the cycle. The strength of the vortex did not rise continuously though, and between $t/T = 0.2$ and 0.3, a slight reduction in circulation was observed, although the cause of this reduction is not directly apparent. Following the peak in strength, the vortex rapidly lost strength, falling to $\Gamma/cU_\infty = 0.32$ at $t/T = 0.68$. The value of circulation then continued to decrease more slowly, reaching a minimum at $t/T = 0.96$, before rapidly rising once more at the beginning of the subsequent cycle. The value of circulation at the trailing edge in static testing[22] was $\Gamma/cU_\infty = 0.4$, and, if a linear vortex strength is assumed along the wing, it may, thus, be assumed that in the static case $\Gamma/cU_\infty \approx 0.32$ at $x/c = 0.8$.

The results show a phase delay between the wing motion and the development of vortex strength of around 90 deg, given that the peak vortex strength was observed at $t/T \approx 0.49$, whereas the peak lateral velocity of the wing occurred at $t/T = 0.25$. This phase delay results in a good correlation between the increase in vortex strength and the jump in the breakdown location. Between $t/T \approx 0.0$ and 0.3, the vortex strength remained relatively constant, and little change in the breakdown location was observed during this period. Between $t/T \approx 0.3$ and 0.5, the vortex strength increased to around $\Gamma/cU_\infty = 0.4$, representing an increase in strength of 20% compared with its initial value. An upstream progression of the breakdown during this period would, therefore, be expected. Finally, between $t/T \approx 0.5$ and 1.0, the vortex weakened to around its original value, and the breakdown showed a slow progression downstream as it attempted to regain its initial location. Thus, the sudden movement of the breakdown upstream may be attributed to the increased magnitude of vortex strength around the midpoint of the cycle.

Conclusions

The particular focus of this investigation has been on the interaction of vortices generated by delta wing models at high angle of attack with support structures. A novel approach was used whereby the effects of time-varying vortex strength could be separated from the effects of the vortex–support interaction.

In the constant vortex strength case with an oscillating dummy support, the magnitude of lift force fluctuations over the wing showed a very similar response to the fluctuations in breakdown location that have been documented previously. The response is that of a first-order low-pass filter, with large magnitude fluctuations at low frequencies, but that decrease as the frequency is increased. A comparison of three forms of dynamic motion showed that the greatest coherence between the oscillating motion and lift force response was observed for the large-amplitude motion.

When the effects of time-varying vortex strength are included, a clearer picture of the overall form of response that may be observed in dynamic testing is obtained. In this case, whereas the breakdown response was similar to that for constant vortex strength at low frequencies, at high frequencies the magnitude of breakdown fluctuations increased. Thus, in terms of the magnitude of breakdown fluctuations, the response is dominated by support interference at low frequencies, whereas at high frequencies it is the effect of changes in vortex strength that dictate the breakdown location. However, note that the effect of support interference was to shift the mean breakdown location upstream at all frequencies because, for the candidate wing configuration, breakdown was not observed in the absence of support interference.

A number of important observations have also been made with regard to the behavior of the vortices at high forcing frequencies. It was noted that the trajectories of the vortices were altered by the movement of the wing, with the vortex on the windward side of the model moving toward the wing surface and the wing centerline, whereas the opposite movement occurred on the leeward side. Significant kinking of the vortex was seen under some conditions, which was related to the change in direction of the wing at the limits of its motion. Most curious was the observation of a jumping of the breakdown location on the windward side of the model at high frequencies. In this case, the breakdown was seen to rapidly progress upstream, to the point where, in some cases, two breakdowns were observed in the flow simultaneously. PIV measurements of the cross-flow plane and subsequent circulation calculations have shown that a rapid increase in vortex strength may be the cause of this phenomenon. The effect of the support was to reduce the magnitude of the breakdown jump, but jumping was nevertheless observed in all of the cases considered at high enough forcing frequencies.

Acknowledgments

This work was funded by the United Kingdom Ministry of Defence, under Package 07b of the Applied Research Programme.

References

[1]Frink, N. T., "Computational Study of Wind-Tunnel Wall Effects on the Flowfield Around Delta Wings," AIAA Paper 87-2420, 1987.

[2]Thompson, S. A., Bathill, S. M., and Nelson, R. C., "Separated Flowfield on a Slender Wing Undergoing Transient Pitching Motions," *Journal of Aircraft*, Vol. 28, No. 8, 1991, pp. 489–495.

[3]Thomas, J. P., and Lan, C. E., "The Simulation and Correction of Wind Tunnel Wall Interference on Delta Wing Lift Using Navier–Stokes and Euler Solutions," AIAA Paper 91-3300, 1991.

[4]Hsing, C.-C. A., and Lan, C. E., "Low-Speed Wall Interference Assessment/Correction with Vortex Flow Effect," *Journal of Aircraft*, Vol. 34, No. 2, 1997, pp. 220–227.

[5]Weinburg, Z., "Effect of Tunnel Walls on Vortex Breakdown over Delta Wings," *AIAA Journal*, Vol. 30, No. 6, 1992, pp. 1584–1587.

[6]Allan, M. R., "A CFD Investigation of Wind Tunnel Interference on Delta Wing Aerodynamics," Ph.D. Dissertation, Dept. of Aerospace Engineering, Univ. of Glasgow, Glasgow, Scotland, U.K., Dec. 2002.

[7]Pankhurst, R. C., and Holder, D. W., *Wind-tunnel technique*, Sir Isaac Pitman and Sons, 1965.

[8]"Blockage Correction for Bluff Bodies in Confined Flows," Engineering and Sciences Data Unit, ESDU, London, Item 80024, 1984.

[9]Ericsson, L. E., and Reding, J. P., "Review of Support Interference in Dynamic Tests," *AIAA Journal*, Vol. 21, No. 12, 1983, pp. 1652–1666.

[10]Ericsson, L. E., and Reding, J. P., "Dynamic Support Interference in High-Alpha Testing," *Journal of Aircraft*, Vol. 23, No. 12, 1986, pp. 889–896.

[11]Perkins, E. W., "Experimental Investigations of the Effects of Support Interference on the Drag of Bodies of Revolution at a Mach Number of 1.5," NACA RM A8B056, May 1948.

[12]Johnson, J. L., Grafton, S. B., and Yip, L. P., "Exploratory Investigation of Vortex Bursting on the High Angle of Attack Lateral Directional Stability Characteristics of Highly Swept Wings," AIAA Paper 80-0463, 1980.

[13]Hummel, D., "Untersuchungen über das Aufplatzen der Wirbel an Schlanken Delta Flügeln," *Zeitschrift für Flugwissenschaften*, Vol. 5, No. 3, 1965, pp. 158–168.

[14]Ericsson, L. E., "Another Look at High-Alpha Support Interference in Rotary Tests," *Journal of Aircraft*, Vol. 28, No. 5, 1991, pp. 584–591.

[15]Beyers, M. E., "Unsteady Wind-Tunnel Interference in Aircraft Dynamic Experiments," *Journal of Aircraft*, Vol. 29, No. 6, 1992, pp. 1122–1129.

[16]Beyers, M. E., and Ericsson, L. E., "Ground Facility Interference on Aircraft Configurations with Separated Flow," *Journal of Aircraft*, Vol. 30, No. 5, 1993, pp. 682–688.

[17]Beyers, M. E., and Ericsson, L. E., "Implications of Recent Rotary Rig Results for Flight Prediction," *Journal of Aircraft*, Vol. 37, No. 4, 2000, pp. 545–553.

[18]Ericsson, L. E., and Beyers, M., "Aspects of Ground Facility Interference on Leading-Edge Vortex Breakdown," *Journal of Aircraft*, Vol. 38, No. 2, 2001, pp. 310–314.

[19]Taylor, G. S., Gursul, I., and Greenwell, D. I., "Investigation of Support Interference in High-Angle-of-Attack Testing," *Journal of Aircraft*, Vol. 40, No. 1, 2003, pp. 143–152.

[20]Beran, P. S., and Culick, F. E. C., "The Role of Non-Uniqueness in the Development of Vortex Breakdown in Tubes," *Journal of Fluid Mechanics*, Vol. 242, 1992, pp. 491–527.

[21]Lowson, M. V., "Some Experiments with Vortex Breakdown," *Journal of the Royal Aeronautical Society*, Vol. 68, 1964, pp. 343–346.

[22]Taylor, G. S., "Support Interference in Oscillatory Dynamic Tunnel Testing," Ph.D. Dissertation, Dept. of Mechanical Engineering, Univ. of Bath, Bath, England, U.K., June 2003.

[23]Polhamus, E. C., "Predictions of Vortex Lift Characteristics by a Leading-Edge Suction Analogy," *Journal of Aircraft*, Vol. 8, No. 4, 1971, pp. 193–199.

[24]Gursul, I., "Proposed Mechanism for the Time Lag of Vortex Breakdown Location in Unsteady Flows," *Journal of Aircraft*, Vol. 37, No. 4, 2000, pp. 733–736.

[25]Guglieri, G., and Quagliotti, F. B., "Experimental Investigation of Vortex Dynamics on a 65° Delta Wing in Sideslip," *Aeronautical Journal*, Vol. 101, March 1997, pp. 111–120.

[26]Verhaagen, N. G., and Naarding, S. H. J., "Experimental and Numerical Investigation of Vortex Flow over a Sideslipping Delta Wing," *Journal of Aircraft,* Vol. 26, No. 11, 1989, pp. 971–978.

[27]Harvey, J. K., "Some Observations of the Vortex Breakdown Phenomenon," *Journal of Fluid Mechanics,* Vol. 14, Pt. 4, Dec. 1962, pp. 585–592.

[28]Sarpkaya, T., "Vortex Breakdown in Swirling Conical Flows," *AIAA Journal,* Vol. 9, No. 9, 1971, pp. 1792–1799.

[29]Hall, M. G., "Vortex Breakdown," *Annual Review of Fluid Mechanics*, Vol. 4, 1972, pp. 195–217.

[30]Gursul, I., and Ho, C., "Vortex Breakdown over Delta Wings in Unsteady Freestream," *AIAA Journal*, Vol. 32, No. 2, 1994, pp. 433–436.

[31]Leibovich, S., "Vortex Stability and Breakdown: Survey and Extension," *AIAA Journal*, Vol. 22, No. 9, 1984, pp. 1192–1206.